Molecular Simulation

ISSN: 0892-7022 (Print) 1029-0435 (Online) Journal homepage: https://www.tandfonline.com/loi/gmos20

Molecular Simulation Study of the Vapor–Liquid Interfacial Behavior of a Dimer-forming Associating Fluid

Jayant K. Singh & David A. Kofke

To cite this article: Jayant K. Singh & David A. Kofke (2004) Molecular Simulation Study of the Vapor–Liquid Interfacial Behavior of a Dimer-forming Associating Fluid, Molecular Simulation, 30:6, 343-351, DOI: 10.1080/08927020310001657108

To link to this article: https://doi.org/10.1080/08927020310001657108

Published online: 21 Aug 2006.

Molecular Simulation, Vol. 30 (6), 15 May 2004, pp. 343–351

Taylor & Francis
Taylor & Francis Group

Molecular Simulation Study of the Vapor–Liquid Interfacial Behavior of a Dimer-forming Associating Fluid

JAYANT K. SINGH and DAVID A. KOFKE*

Department of Chemical and Biological Engineering, University at Buffalo, The State University of New York, Buffalo, NY 14260-4200, USA

(Received July 2003; In final form December 2003)

Grand-canonical transition-matrix Monte Carlo simulation is applied to analyze the effect of molecular association on the vapor–liquid coexistence and interfacial behavior of square-well based dimerizing fluids. Finite-size scaling techniques are implemented in conjunction with histogram reweighting to determine the infinite-system surface tension from a series of finite-size simulations. The effect of strength of association and size of association site on coexistence densities, pressure, surface tension, and monomer fraction is presented. Some qualitative features of the dependence of monomer fraction and surface tension on association strength are found to disagree with behavior expected from previous studies using the statistical associating fluid theory (SAFT). Comparison with experimental data shows that molecular models must incorporate an explicit association interaction in order to describe the surface-tension behavior of a real dimerizing fluid (acetic acid).

Keywords: Surface tension; Associating fluids; Transition-matrix Monte Carlo

INTRODUCTION

The behavior of liquids and vapors in contact is of fundamental scientific and technological importance. In recent years, development of new modeling tools and techniques and increase in computing power has facilitated the theoretical study of interfacial phenomena. Some theoretical developments such as integral equation methods, density gradient theory and density functional theory (DFT) can be used for the study of inhomogeneous materials. For the vapor–liquid interface in particular, DFT and density gradient theory are popular approaches. Recently, these methods have been combined with the statistical associating fluid theory (SAFT) to study complex systems [1–4] and model potentials [5]. As with any molecular-based theoretical method, the study of interfacial behavior of model potentials via SAFT can benefit from companion studies involving molecular simulations. Simulation studies are useful in identifying the strengths and deficiencies in a theory, leading to its targeted improvement for better understanding the behavior of real fluids. Simulations are also useful in probing the thermophysical behavior of model systems, and the application of molecular simulation to the study of vapor–liquid interfacial phenomena has attracted a fair amount of attention in recent years [6–10].

Several quantities are of interest with regard to interfacial behavior. Simulation can provide a detailed picture of the transition from one phase to another across the interface, for example. However, in this study, we focus mainly on the surface tension, and consider how it is affected by molecular association, i.e. strong, short-ranged, orientationally dependent interactions between molecules, such as those due to hydrogen bonding. We consider a simple model with square-well type attractions, to gauge the effect of basic features of the association potential on the interfacial tension. For this calculation, we apply a method given by Binder [11], and further developed by Errington [12]. In this approach, grand canonical simulations are used to calculate the free energy barrier between the liquid and vapor phases for series of system sizes. Finite-size scaling is used to extrapolate the infinite-system-size free energy. The method is

*Corresponding author. E-mail: kofke@eng.buffalo.edu

ISSN 0892-7022 print/ISSN 1029-0435 online © 2004 Taylor & Francis Ltd
DOI: 10.1080/08927020310001657108

useful here because, unlike methods based on evaluation of the pressure tensor, the anisotropic association potential does not complicate it. The method works well even in the vicinity of the critical point.

The rest of this paper is organized as follows: in the next section, we briefly describe the method used in this study for calculating the surface tension by molecular simulation. In the third section, the details of simulations are presented and in the fourth section, the results are presented and discussed. We conclude in the fifth section.

MODEL AND METHODS

We study a model due to Chapman [13], modified slightly to treat the isotropic van der Waals interactions with a square well rather than a Lennard–Jones potential. Association is modeled using an orientationally dependent square-well attraction. Each atom has associated a direction vector, and one can imagine a cone surrounding this vector, extending some distance from the surface of the core, such that two atoms with properly oriented overlapping cones will interact with an associative attraction. Specifically, the potential is:

$$u(r_{ij},\theta_i,\theta_j)=\begin{cases}\infty, & 0<r_{ij}<\sigma\\ u_{\mathrm{af}}(\theta_i,\theta_j) & \sigma\le r_{ij}<r_{\mathrm{c}}\sigma\\ -\varepsilon, & r_{\mathrm{c}}\sigma\le r_{ij}<\lambda\sigma\\ 0, & r_{ij}\ge\lambda\sigma\end{cases}$$

$$u_{\mathrm{af}}(\theta_i,\theta_j)=\begin{cases}-\varepsilon_{\mathrm{af}} & \text{if } \theta_i<\theta_{\mathrm{c}} \text{ and } \theta_j<\theta_{\mathrm{c}}\\ -\varepsilon, & \text{otherwise}\end{cases}$$

where θ_i and θ_j are angles between the center-to-center vector and the direction vectors on the respective atoms i and j, $\varepsilon_{\mathrm{af}}$ is the well depth of the attractive cone, $\lambda\sigma$ is the square-well potential diameter, ε is the depth of the isotropic well, and σ is the diameter of hard core. We adopt units such that σ and ε are unity. In this study, we use $\theta_{\mathrm{c}}=27^\circ$ and $\lambda=1.5$. We examine attractive interaction strengths $\varepsilon_{\mathrm{af}}$ ranging from 4.0 to 8.0, with r_{c} ranging 1.05 to 1.20; from a previous study [14] we have also data for a simple non-associating square well model, which corresponds to $\varepsilon_{\mathrm{af}}=1.0$.

This is a single-site model in which each molecule is capable of forming a specific association with only one other molecule. Thus the largest associating cluster that can be formed is a dimer (except for non-specific association due to the spherical square–well interaction). In this regard the model has the same qualitative association behavior as a carboxylic acid.

Surface tension can be evaluated by molecular simulation using one of two general methods. In the first, the surface tension is related to the difference in the normal stresses parallel and perpendicular to a vapor–liquid interface. The stresses can be measured in several ways, all of which have complications when applied to the association model we use. The potential is discontinuous, so to measure the virial tensor we would need to evaluate correlation functions in different directions, and extrapolate–interpolate to the point of discontinuity, as a function of separation and orientation of the molecules. Instead we could use volume perturbations, scaling the length of the box in different directions, and evaluate the pressure tensor elements by measuring the corresponding change in energy and averaging as a free-energy perturbation. We have found this approach to give poor results [14]. Finally, we could perform collision-based molecular dynamics, and measure the impulses associated with each collision. This process is complicated by the anisotropic nature of the potential, and the need to detect collisions that consider the rotation of the molecules as well as their translational movement.

The second approach measures the surface tension through its definition as an interfacial free energy. Binder [11] has shown how measurement of the free energy as a function of density, taken through the two-phase region, can be used within a finite-size scaling formalism to obtain the surface tension for an infinite-sized system. Binder's formalism does not require setting up an explicit interface; rather it relies on spontaneous fluctuations that give rise to density inhomogeneities which provide information regarding the interfacial properties. Such an approach naturally lends itself to application near the critical point, where the necessary fluctuations are sufficiently large, and where maintenance of a well-defined interface causes difficulty for the explicit–interface methods. Errington has demonstrated how histogram reweighting of results from transition–matrix Monte Carlo (TMMC) simulations in the grand-canonical (GC) ensemble can be effective in measuring the free-energy versus density profile. Errington's method can be applied equally well to any model potential, so we have selected it to use for this study. This method has been detailed elsewhere [12], so we provide only an overview of it here.

Grand-canonical Monte Carlo (GCMC) simulation provides fluctuations in number density ($\rho=N/V$) through fluctuations in the particle number N. For subcritical temperatures, the typical form of this distribution is a double peak structure [15,16]. The peaks correspond to pure phases, while the trough in the probability at intermediate densities corresponds to a set of both homogeneous and heterogeneous (interfacial) configurations.

As the system size becomes large, intermediate-density heterogeneous configurations far outweigh homogeneous ones, and the ratio of the density–probability distribution at the intermediate minimum relative to the (mutually equal) peak densities represents the interfacial free energy [11]. For a finite system of characteristic size L, the interfacial free energy is

$$\beta F_L = \frac{1}{2}\left(\ln \Pi^l_{N\max} + \ln \Pi^v_{N\max}\right) - \ln \Pi_{N\min}$$

where Π_N is the probability to observe a system with N particles in a GC simulation; "max" and "min" refer to the values of N where the probability is at an extremum, and the superscripts l and v indicate probability values for the liquid and vapor peaks, respectively (these should be equal, but we use their average to minimize effects of an imperfect equality). From the formalism of Binder, the surface tension for a finite-size three-dimensional system is given by

$$\beta\gamma_L = \frac{\beta F_L}{2L^2} = C_1\frac{1}{L^2} + C_2\frac{\ln L}{L^2} + \beta\gamma_\infty \qquad (1)$$

where γ_∞ is the infinite system ($L \to \infty$) interfacial tension and C_1 and C_2 are constants. Measurements of F_L for increasing L permits extrapolation to infinite size via this formula.

A visited-states method measures the GC probabilities Π by observing their distribution of occurrence in a GCMC simulation. Instead, Errington advocates the TMMC method [17], which measures the probabilities for transitions between macrostates differing in N. The transitions form a Markov process, and the limiting distribution (the Π values) can be evaluated from the transition matrix. One advantage of this approach is that we can apply an N-dependent sampling bias and modify it throughout the simulation without having to rezero or renormalize the TM averages. The method monitors the acceptance probability of attempted MC trials and subsequently uses this information (including trials that are not accepted) to calculate the macrostate transition probability matrix. In the present circumstances, the analysis is simplified because we permit macrostate transitions $N \to N$, $N \to N+1$, and $N \to N-1$ only, so the transition matrix is tri-diagonal. An N-dependent sampling bias is needed to ensure that the simulation provides good statistics for the low-probability macrostates corresponding to the interfacial densities. A reasonable choice is to set the weights η_N equal to the inverse of current estimate of the macrostate probabilities, i.e. $\eta_N = -\ln \Pi_N$. To the extent that this equality holds, the simulation will sample all densities with equal probability.

Another important element of this study is the use of the histogram reweighting method of Ferrenberg and Swendson [18] to evaluate the phase–coexistence value of the chemical potential. This determination is readily performed from knowledge of the probability distribution Π_N from the TMMC calculations [12]. The probability distribution for any other chemical potential is calculated using the following relationship,

$$\ln \Pi_N(\mu) = \ln \Pi_N(\mu_o) + \beta(\mu - \mu_o)N$$

To determine the coexistence chemical potential, we apply the above relation to find the value that produces a probability distribution Π^{coex}_N where the areas under the vapor and liquid regions are equal. Phase densities are calculated from the first moment of the Π^{coex}_N distribution over an appropriate range of N for each phase. Calculation of the saturation pressure can be accomplished through the role of the pressure as the thermodynamic potential in the GC ensemble, which leads to the following expression [19].

$$\beta\rho V = \ln\left(\sum_N \frac{\Pi^{\text{coex}}_N}{\Pi^{\text{coex}}_o}\right) - \ln\ 2 \qquad (2)$$

Simulation of strongly associating systems, such as that examined here, can be troubled by poor sampling. This arises because configurations where molecules are associated may be difficult to find through random sampling, yet they are important because of their favorable energy. Similarly, bound molecules may be only rarely separated through the usual MC trials. This problem can be remedied through the use of association-bias trials in the MC process. We conduct trials in which we preferentially place one molecule in a small box centered on another, or we preferentially select a pair of bound molecules and separate them, and we modify the acceptance probability to remove the bias. The recipe for the association bias method is detailed elsewhere [20]. We also apply this bias for GC insertion/deletion trials. The following is a brief description of the algorithm, which follows the basic idea behind the association-bias displacement trial [20]. Select with equal probability whether to perform bias-insert trial or bias-delete trial; then:

1. *Bias-insert trial*
   a. Choose a molecule A uniformly from the N molecules being simulated.
   b. Place a new molecule B in the bonding region of molecule A.
   c. Rotate the molecule randomly on unit sphere.
2. *Bias-delete trial*
   a. Select a molecule A uniformly from among the bonded molecules (if none are bonded then the trial is rejected). Remove the molecule.

Using detailed balance and the distribution of the GC ensemble, the acceptance probability for this trial is

$$\chi = \exp\left(-\beta(\Delta u - \mu)\right)\frac{\phi V 4\pi}{nN_a}$$

where ϕ is the fraction of simulation volume occupied by a bonding region, N_a is the number of bonded molecules, n is the number of molecules associated with the insertion molecule, Δu is the energy change, μ is the chemical potential. In the current study, we use a cubic bonding volume of edge 2.5 centered on the square-well atom.

SIMULATION DETAILS

We performed molecular simulations using the model and methods described above. Trials were performed with frequency 1:1:2:7:3 for displacement, rotation, bias displacement, insert–delete, bias insert–delete moves. Multiple processors (from 16 to 256) were used in parallel for large box sizes, in which different processors were dedicated to simulation of systems for different ranges of N [21]. We applied thread based parallelization using the molecular simulation software package *Etomica* [22,23], and the message passing interface in Java (mpiJava) [http://www.hpjava.org/mpiJava.html] for this purpose. Bias weights η_N were updated after every million MC trials. The length of the runs ranged from 50 to 100 million trials, depending on the simulation box size. Four block subaverages of the measured macrostate transition matrix were taken for calculating the confidence limits. Coexistence properties were calculated using a box size $L = 10$. Surface tensions were calculated using the finite size scaling method, with values of box size $L = 8$, 9, 10, 12 and 14. For the largest of these systems up to 1968 atoms were simulated. In order to speed up the calculation a cell-based neighbor list scheme was applied. Critical properties were calculated a using rectilinear diameter approach [14].

RESULTS AND DISCUSSION

Figure 1 shows the temperature–density coexistence envelope of the model studied here, for various strengths of attraction. These properties are calculated at a fixed cutoff $r_c = 1.05$ for the associating site. The effect of association on coexistence properties becomes noticeable at higher strengths of attraction ($\varepsilon_{af} \geq 6$). The general effect of association is to increase the density of the liquid and decrease the density of the vapor. For the liquid the density increase results from the promotion of more compact arrangements of the molecules; for the vapor the decrease in density results from a lowering of the vapor pressure with increasing association. The general effect of association is to raise the critical temperature.

The monomer fraction is defined as the fraction of all molecules that are not bonded to another molecule. Figure 2 shows the variation of the monomer fraction with strength of attraction. The figure shows that the liquid monomer fraction decreases markedly at lower temperature, especially for $\varepsilon_{af} = 8.0$ and $\varepsilon_{af} = 6.0$. In the vapor there is almost no association (nearly 100% monomer) for $\varepsilon_{af} < 8.0$. To the extent it is present, association in the vapor increases with temperature (monomer fraction decreases), which

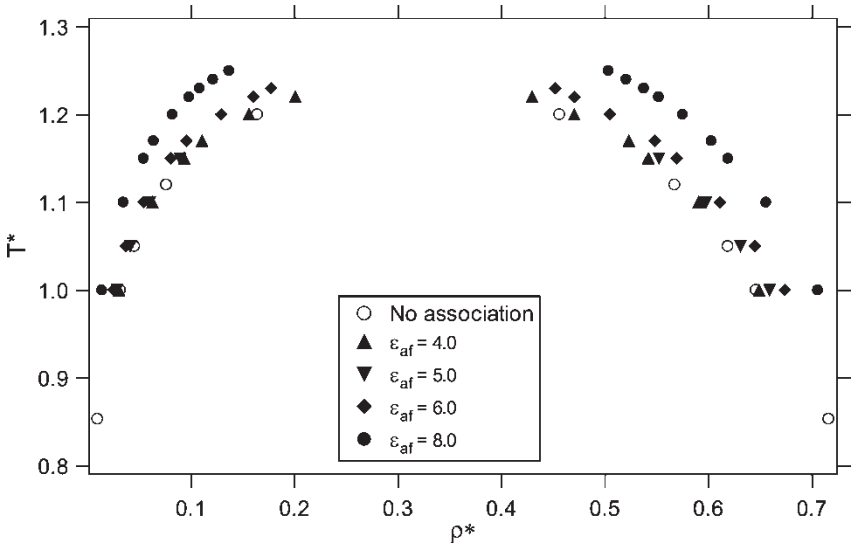

FIGURE 1 Temperature–density coexistence envelope of square-well based associating fluids. Site size (cutoff for associating site) is fixed at $r_c = 1.05$. The behavior is compared with no-association model ($\varepsilon_{af} = 1.0$) [14]. Error bars are smaller than the symbol size. Reduced units are $T^* = kT/\varepsilon$, $\rho^* = \rho\sigma^3$.

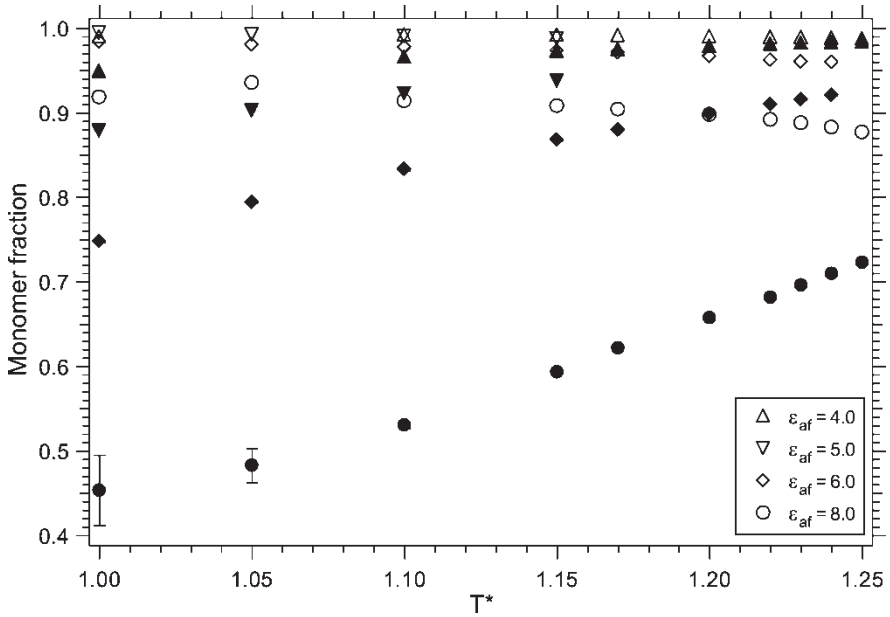

FIGURE 2 Monomer fraction of square-well based associating fluids. Site size (cutoff for associating site) is fixed at $r_c = 1.05$. Open and filled symbols represent data for vapor and liquid phases, respectively. Reduced units are $T^* = kT/\varepsilon$.

occurs because the (coexistence) pressure also increases in this direction. This behavior is in contrast with that predicted by a SAFT treatment applied to a similar (but not identical) model: SAFT indicates that both monomer fractions—liquid and vapor—increase with temperature [1]. The difference between liquid and vapor monomer fractions increases at a given temperature with an increase in the strength of attraction, indicating that the effect is greater on the condensed phase than on vapor phase. As the temperature increases toward the critical point, the difference in liquid and vapor monomer fraction decreases, as it must because liquid and vapor phases are approaching each other.

Figure 3 shows the saturated vapor pressure in a Clausius–Clapeyron plot for various values of association energy. As expected, the saturation pressure decreases as the association strength increases, and no curvature is evident in any of the plots. There is a small increase (becoming more negative)

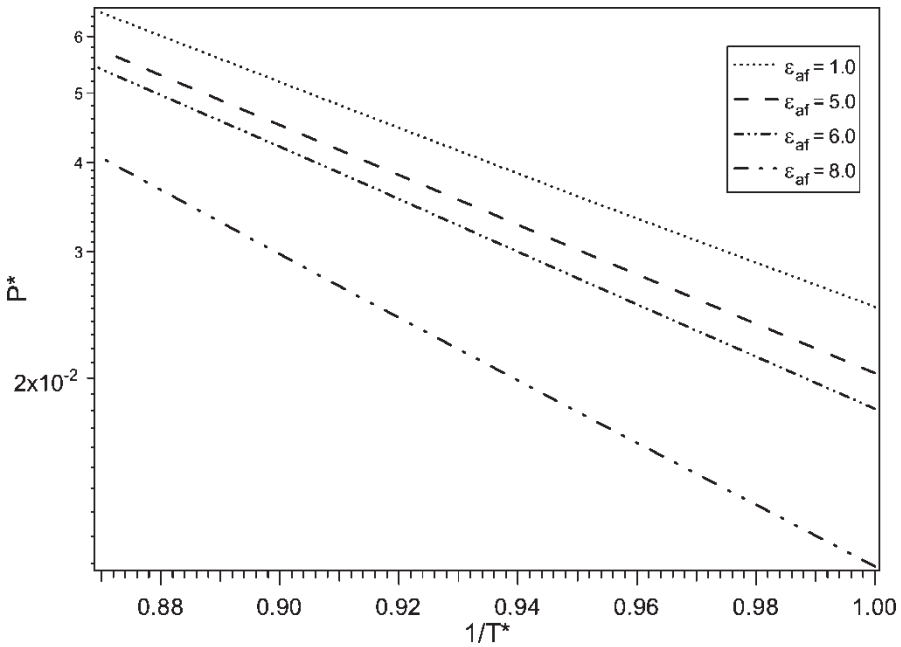

FIGURE 3 Vapor pressure of the associating fluids as a function of the inverse temperature. The values for $\varepsilon_{af} = 1.0$ are taken from Ref. [14]. Reduced units are $T^* = kT/\varepsilon$, $P^* = P\sigma^3/\varepsilon$.

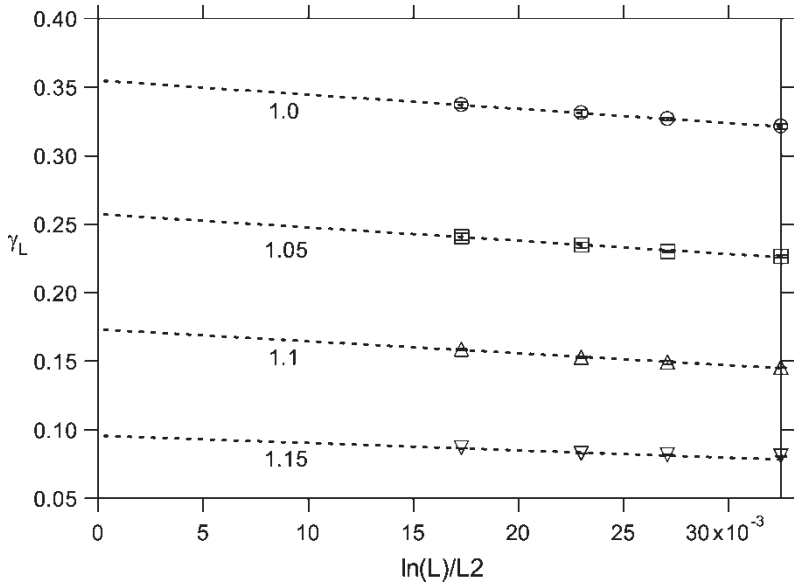

FIGURE 4 The system size dependence of the surface tension for the system with $\varepsilon_{af} = 5.0$ and $r_c = 1.2$. The dashed lines show the linear extrapolation to infinite system size. L is the edge length of the cubic simulation box. Temperature T^* is indicated by the value with each line.

in the slope of the curve with increasing association strength. This variation is connected primarily to the change in the enthalpy of vaporization. Association in the vapor tends to diminish the heat of vaporization, while that in the liquid increases it. That it increases with ε_{af} reflects the greater response of the liquid monomer fraction to increasing association strength, in comparison to the vapor.

Figure 4 shows typical results for the interfacial free energy as a function of system size, presented for extrapolation to an infinite system according to Eq. (1). The plot shows that the results are precise, that their confidence limits are much smaller than the variation with system size, which in turn is much smaller than the variation with temperature. The data have the anticipated linear dependence with $\ln(L)/L^2$, and there is reason to have confidence in the extrapolated results. Figure 5 shows these infinite-system extrapolations as a function of temperature for various values of strength of attraction. As expected, the surface tension increases with the increase in the strength of

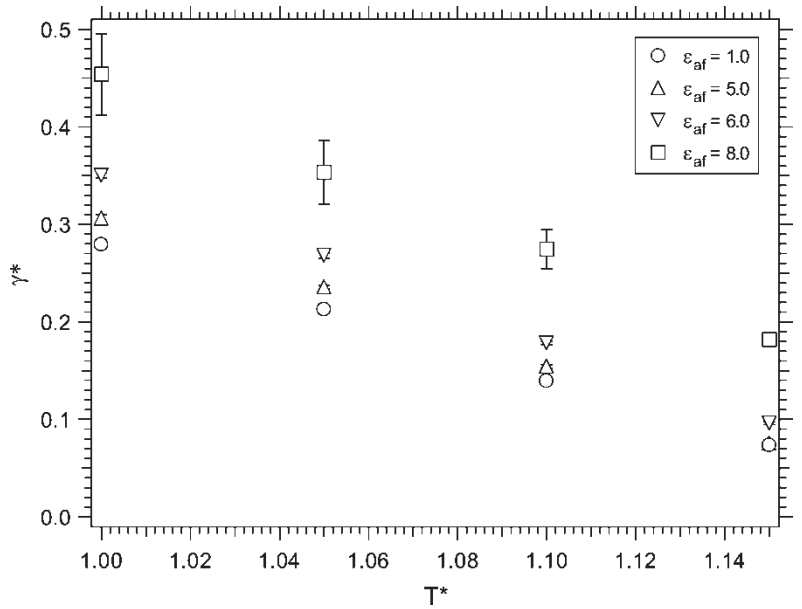

FIGURE 5 Surface tension of square-well based associating fluids. Site size (cutoff for associating site) is fixed at $r_c = 1.05$. The surface tension for non-associating square-well model is taken from Ref. [14]. Reduced units are $T^* = kT/\varepsilon$, $\gamma^* = \gamma\sigma^2/\varepsilon$.

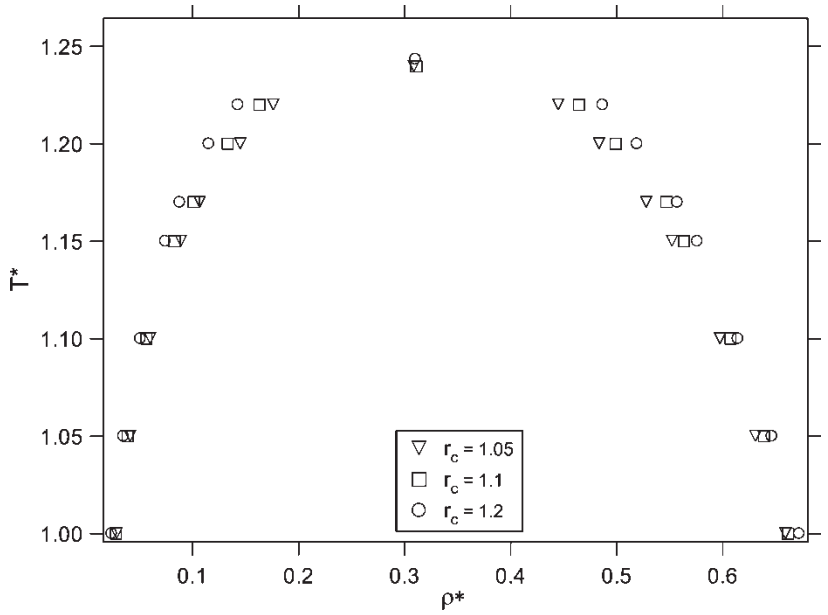

FIGURE 6 Coexistence vapor and liquid densities of associating fluid for three values of associating site sizes. The value of associating strength is fixed at $\varepsilon_{af} = 5.0$.

attraction and decreasing temperature. There is no discernable curvature in these plots, which are still somewhat removed from the critical temperature. The slope of the surface tension versus temperature does not show any strong dependence on the association strength—the curves are nearly parallel. SAFT calculations [1] have indicated a significant dependence of these slopes on the association strength (again, for a similar but nevertheless different model).

We now turn to consider the effect of the size of the association site for fixed association strength. Figure 6 shows the coexistence properties for $\varepsilon_{af} = 5.0$ while varying the size of the site via r_c. The effect is surprisingly small, and to the extent it is present it is more prominent at higher temperature than at lower temperature. Yet the critical point is not much affected by the size. Despite the insensitivity of coexistence properties to association-site size, the monomer fraction does change drastically, as shown

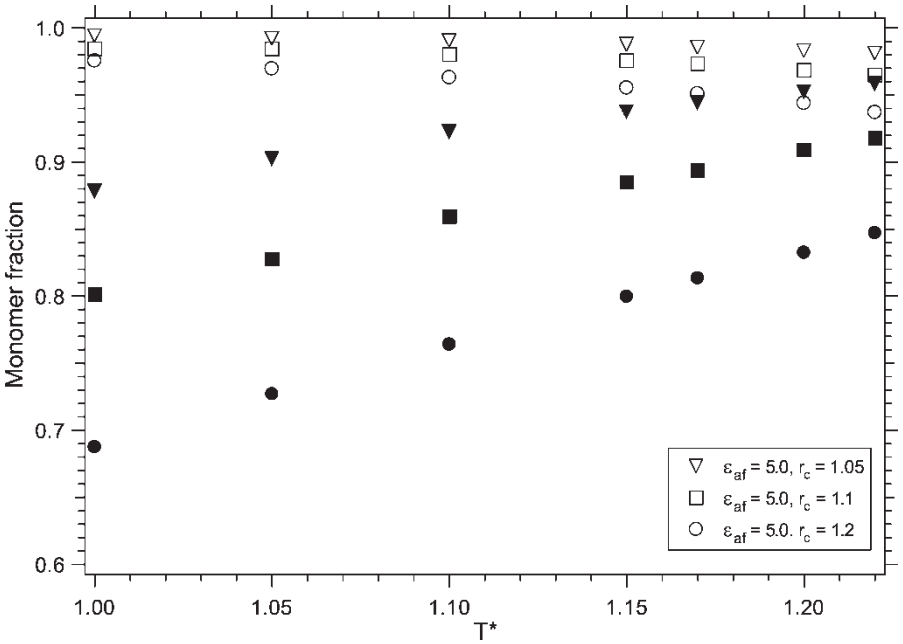

FIGURE 7 Monomer fraction of associating fluid for three values of associating site sizes. The value of associating strength is fixed at $\varepsilon_{af} = 5.0$. Open symbols represent data for vapor phase and filled symbols represent data for condensed phase. Reduced units are $T^* = kT/\varepsilon$.

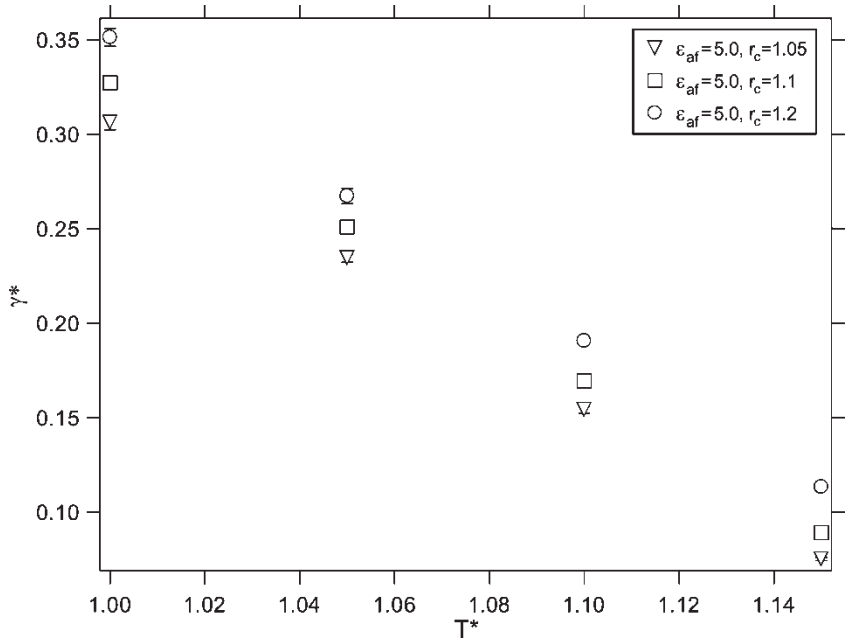

FIGURE 8 Surface tension as a function of temperature for three values of associating site sizes. The value of associating strength is fixed at $\varepsilon_{af} = 5.0$.

in Fig. 7. The effect is most pronounced at a lower temperature. The difference in the monomer fraction of liquid and vapor increases at a given temperature as one increases the size of the site. This behavior is reflected in the surface tension, as shown in Fig. 8. Thus, we have the interesting result that the effect of the size of the site is greater on interfacial tension (which varies by 17–50% over the range of site sizes) than on the coexistence properties (where the densities vary by only 2–9% over the same range). The surface tension change is uniform as the size of the site increases. The slope of the curve at various values of cutoff of associating site is more or less the same, indicating that surface tension increases by some constant amount with respect to temperature regardless of the site size.

Finally, we compare all the model surface tension values with experimental data for several real

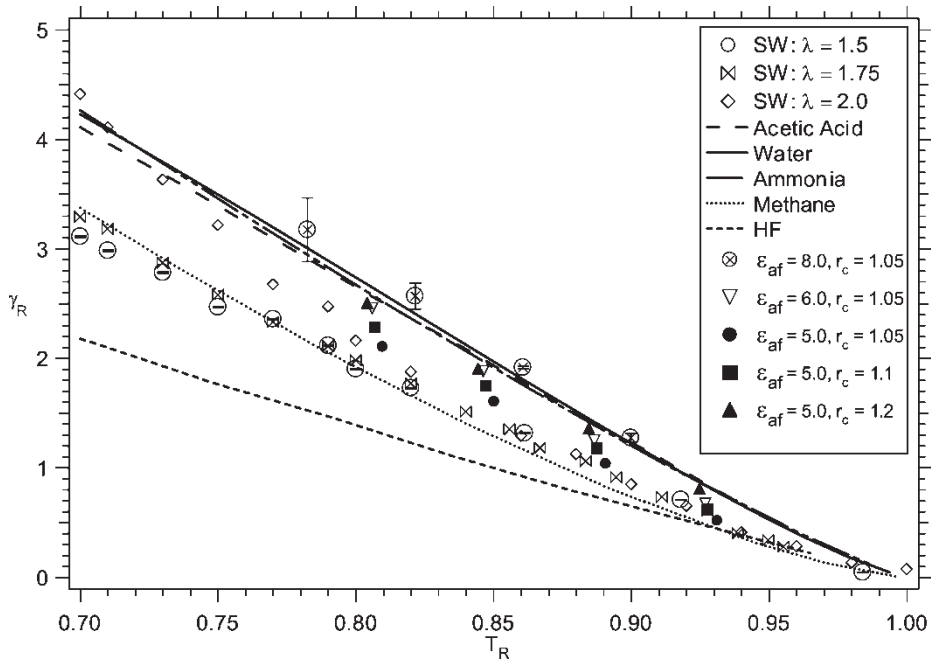

FIGURE 9 Comparison of surface tension of model fluids with experimental data for real fluids [24], as a function of temperature. Results labeled "SW" are for a non-associating square-well model with well-extent parameter λ as indicated. Values are reduced by critical properties: $\gamma_R = \gamma\rho_c^{1/3}/P_c$ and $T_R = T/T_c$.

associating (ammonia, water, acetic acid, and hydrogen fluoride) and non-associating (methane) fluids in a corresponding-states plot, with quantities reduced by the critical temperature, pressure, and density (Fig. 9). It is interesting to see that when presented this way, the non-associating model (simple square well, $\varepsilon_{af} = 1.0$) significantly underestimates the surface tension of water and acetic acid. Moreover, variation of the isotropic square-well range of attraction does not satisfactorily improve the comparison with the experiment. In contrast, addition of the association site moves the surface tension up, in a way that permits good agreement with the acetic-acid curve for $\varepsilon_{af} = 5.0$ and $r_c = 1.2$. Acetic acid forms dimers, and it is gratifying to see that incorporation of this feature in the model helps in matching the experimental data. On the other hand, the surface tension of water is also in this vicinity, and water forms more complex aggregates than dimers, while the surface tension of methane is in general agreement with the curve for the non-associating $\lambda = 1.5$ square-well model; in both of these cases the general agreement between the models and experiment must be considered fortuitous. No model parameters are able to approximate hydrogen fluoride behavior, which has an anomalously low surface tension. These results suggest a more complicated model is required which can capture the formation of oligomer chains and rings, especially in the vapor phase.

CONCLUSIONS

The methodology advocated by Errington for measuring surface tensions by molecular simulation is effective for application to associating fluids, provided an association bias method is used to enhance sampling of associating clusters in the vapor. The method relies on Binder's finite-size scaling of the surface free energy as measured in the grand canonical ensemble, coupled with the TMMC and histogram reweighting methods. We examined the effect of the strength and size of the association site on the thermodynamic properties of a model dimerizing fluid. The interfacial tension is sensitive to both the size of the associating sites and the strength of the association, while the coexistence properties are sensitive more to the strength rather than the size of the site. The current model with moderate association energy is capable of describing qualitatively the behavior of a real dimerizing fluid like acetic acid, whereas models not including explicit association interactions cannot describe this behavior as satisfactorily.

Acknowledgements

This work has been supported by the U.S. National Science Foundation, grant CTS-0076515. Computational resources have been provided by the University at Buffalo Center for Computational Research. We thank Jeffrey Errington for his advice in implementing the methodology for the surface-tension calculations.

References

[1] Blas, F.J., del Rio, E.M., de Miguel, E. and Jackson, G. (2001) "An examination of the vapour–liquid interface of associating fluids using a SAFT-DFT approach", *Mol. Phys.* **99**, 1851.
[2] Kahl, H. and Enders, S. (2000) "Calculation of surface properties of pure fluids using density gradient theory and SAFT-EOS", *Fluid Phase Equil.* **172**, 27.
[3] Kahl, H. and Enders, S. (2002) "Interfacial properties of binary mixtures", *Phys. Chem. Chem. Phys.* **4**, 931.
[4] Lu, J.-F., Fu, D., Liu, J.-C. and Li, Y.-G. (2002) "Application of density functional theory for predicting the surface tension of pure polar and associating fluids", *Fluid Phase Equil.* **194–197**, 755.
[5] Gloor, G.J., Blas, F.J., del Rio, E.M., de Miguel, E. and Jackson, G. (2002) "A SAFT-DFT approach for the vapour–liquid interface of associating fluids", *Fluid Phase Equil.* **194–197**, 521.
[6] Orea, P., Duda, Y. and Alejandre, J. (2003) "Surface tension of a square well fluid", *J. Chem. Phys.* **118**, 5635.
[7] Chen, B., Siepmann, J.I., Oh, K.J. and Klein, M.L. (2001) "Aggregation-volume-bias Monte Carlo simulations of vapor–liquid nucleation barriers for Lennard–Jonesium", *J. Chem. Phys.* **115**, 10903.
[8] Moody, M.P. and Attard, P. (2001) "Curvature dependent surface tension from a simulation of a cavity in a Lennard–Jones liquid close to coexistence", *J. Chem. Phys.* **115**, 8967.
[9] Potoff, J.J. and Panagiotopoulos, A.Z. (2000) "Surface tension of the 3-dimensional Lennard–Jones fluid from histogram-reweighting Monte Carlo simulations", *J. Chem. Phys.* **112**, 6411.
[10] Mecke, M., Winkelmann, J. and Fischer, J. (1997) "Molecular dynamics simulation of the liquid–vapor interface: the Lennard–Jones fluid", *J. Chem. Phys.* **107**, 9264.
[11] Binder, K. (1982) "Monte Carlo calculation of the surface tension for two- and three-dimensional lattice gas models", *Phys. Rev. A* **25**, 1699.
[12] Errington, J.R. (2003) "Evaluating surface tension using grand-canonical transition-matrix Monte Carlo simulation and finite-size scaling", *Phys. Rev. E* **67**, 012102.
[13] Chapman, W.G. (1990) "Prediction of the thermodynamic properties of associating Lennard–Jones fluids: theory and simulation", *J. Chem. Phys.* **93**, 4299.
[14] Singh, J.K., Kofke, D.A. and Errington, J.R. (2003) "Phase coexistence and surface tension of square-well of varying well extent", *J. Chem. Phys.* **119**, 3405.
[15] Hill, T.L. (1962) *Thermodynamics of Small Systems, Parts I and II* (Dover, New York).
[16] Wood, W.W. (1968) "Monte Carlo calculations for hard disks in the isothermal-isobaric ensemble", *J. Chem. Phys.* **48**, 415.
[17] Fitzgerald, M., Picard, R.R. and Silver, R.N. (1999) "Canonical transition probabilities for adaptive metropolis simulation", *Europhys. Lett.* **46**, 282.
[18] Ferrenberg, A.M. and Swendsen, R.H. (1988) "New Monte Carlo technique for studying phase transitions", *Phys. Rev. Lett.* **61**, 2635.
[19] Errington, J.R. and Panagiotopoulos, A.Z. (1998) "Phase equilibria of the modified Buckingham exponential-6 potential from Hamiltonian scaling grand canonical Monte Carlo", *J. Chem. Phys.* **109**, 1093.
[20] Wierzchowski, S. and Kofke, D.A. (2001) "A general-purpose biasing scheme for Monte Carlo simulation of associating fluids", *J. Chem. Phys.* **114**, 8752.
[21] Singh, J.K., Kofke, D.A., Errington, J.R. and Jones, M.D. (2003) in preparation.
[22] Kofke, D.A. and Mihalick, B.C. (2002) "Web-based technologies for teaching and using molecular simulation", *Fluid Phase Equil.* **194–197**, 327.
[23] Kofke, D.A. (2003) *Chem. Eng. Ed.*, Submitted.
[24] Beaton, C.F. and Hewitt, G.F. (1989) *Physical Property Data for the Design Engineer* (Hemisphere, New York).